Comparison of Direct Variogram Upscaling and Scaling Laws

M. Cuba, O. Babak and O. Leuangthong

Mineral deposits resource models in mining as well as reservoirs models in petroleum are built in a bigger scale from sampled data. Resource models are the combinations of different physical or geological events that make the environment to be modeled a very non stationary phenomenon. The bigger scaled block sizes in the model capture those behaviors from the combination of those domains into the block (see Figure 1). In such cases calculation of upscaled semivariograms could be a very difficult task to perform. From the point scale simulated model it is possible to evaluate the mineral deposit for different block sizes and configurations taking into account the effect of the domain contacts on them. On the other hand in the petroleum context there is no presence of small structures that have to be modeled separately and reproduction of domain contacts in the upscaled blocks are not important as in the mining context are. The present exercises then considers big domains that can be modeled with one semivariogram model and there is enough information after upscaling for calculating semivariogram reproduction at different scales.

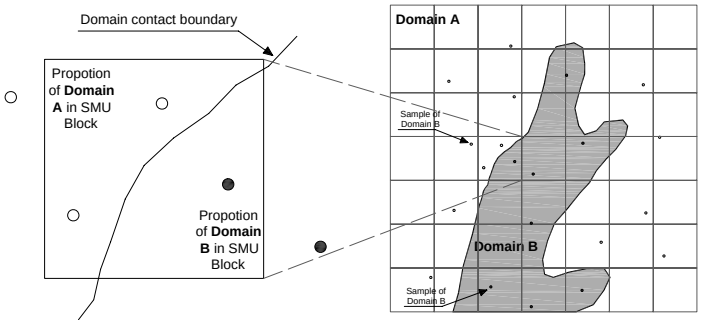

Figure 1: combination of different domains in a SMU scale usually present in mineral deposits

There are many theoretical approaches for semivariogram model scaling, as mentioned by O. Babak and O. Leuangthong 2008 the scaling laws associated with the semivariogram are known from Journel and Huibregts 1978, Frykman and Deutsch 1999, 2002. They showed that it is possible to predict how the semivariogram model of the initial data usually at a point scale changes as the volume of estimation / simulation changes under what they call scaling laws that are based on certain assumptions, one of those assumptions are the invariability in the shape of the upscaled semivariogram models. Also M. David 1977 showed the smoothing or upscaling process and how it affects the semivariogram model reproduction. He showed one dimensional examples upscaling the length of the samples and their respective changes both in the semivariogram model and the experimental semivariogram and how the shape of the changes with the scale of the sample.

O. Babak and O. Leuangthong 2008 propose direct semivariogram upscaling which is numerical approximation of semivariogram model upscaling that is not supported under the previous mentioned scaling laws neither on their assumptions. Some of the important features of their approach are that after upscaling the resulting semivariogram model loses any nugget effect since it vanishes in the process and the semivariogram model shape tend to change to a Gaussian semivariogram model shape.

In a second order stationary environment the direct semivariogram upscaling approach fits better to the resulting semivariogram models than the traditional approach of scaling laws. Most of the information for petroleum reservoir evaluation comes from wells and in mining from exploratory drilling campaigns in both cases the samples are assumed to be in a pseudo point scale due to their relative volumes compared between the models and sampling. Under the statement of the nugget effect vanishes product of upscaling if would lead to think that any nugget effect present in the pseudo point scale which is the initial sampling would disappear after drilling compositing. Practice in mining has shown that compositing rather than eliminating the nugget effect it is reduced as the compositing length increases. It is important to address this point because in most of the cases in the sub groups of datasets as a result of domaining the impact of second order non stationary is still significant.

The present document shows a comparison between the traditional semivariogram scaling laws and the direct semivariogram upscaling approaches in four exercises. On each of the four exercises the latest approach has the

better prediction of the upscaled semivariogram model based on squared error criteria of the experimental semivariogram values and the predicted semivariogram model. The first and the second exercises are a one dimensional and a two dimensional synthetic cases respectively, the third exercise is a two dimensional case with presence of conditioning data (amoco2D.dat), and the fourth last exercise is a three dimensional case with the input data part of a porphyry copper deposit.

Variogram Upscaling

Variogram models are scale dependant, that is, variogram models change as geostatistical model support changes. To represent the volume support of interest, the variogram models need necessarily be scaled. There are two approaches that can be used for this purpose. These are variogram scaling laws approach (Journel and Huijbregts 1978; Frykman and Deutsch 1999, 2002) and theoretically derived direct variogram upscaling approach (Babak and Leuangthong 2008). A short description of both approaches follows.

The variogram scaling laws approach is the most common method for predicting how the semivariogram model changes as the support volume in the geostatistical model changes. This approach focuses on the change in the nugget effect, range and contributions of each nested structure in the semivariogram model with the change in the model support. Specifically, if $\gamma_v(\mathbf{h})$ is a semivariogram model at arbitrary scale *v*:

$$\gamma_v(\mathbf{h}) = C_v^0 + \sum_{m=1}^{k} C_v^m \gamma_v^m(\mathbf{h}) \tag{1}$$

Where C_v^0 is the nugget effect, *k* is the number of nested variogram structures used to fit the experimental variogram of the data, $C_v^m, \quad m = 1,\ldots,k,$ is the variance contribution of each nested structure, and $\gamma_v^m(\mathbf{h}), \quad m = 1,\ldots,k,$ are individual nested variogram structures with sill of one. Each nested structure is given by analytical function (e.g., spherical, exponential, etc.). Then, it follows from the scaling laws that a semivariogram model $\gamma_V(\mathbf{h})$ at a larger volume *V*, where $v \subset V$, is given by

$$\gamma_V(\mathbf{h}) = C_V^0 + \sum_{m=1}^{k} C_V^m \gamma_V^m(\mathbf{h}), \tag{2}$$

Where C_V^0 is the nugget effect, $C_V^m, \quad m = 1,\ldots,k,$ is the variance contribution of each nested structure, and $\gamma_V^m(\mathbf{h}), \quad m = 1,\ldots,k,$ are individual nested variogram structures (all for the scale *V*). The upscaled variogram parameters are calculated as follows (Journel and Huijbregts 1978; Oz and Deutsch 2002):

1. If a_v^m is the range of $\gamma_v^m(\mathbf{h}), \quad m = 1,\ldots,k,$ for the small scale, then the range a_V^m of $\gamma_V^m(\mathbf{h}), \quad m = 1,\ldots,k,$ for the large scale is given by

$$a_V^m = a_v^m + (|V| - |v|) \tag{3}$$

   Where |*V*| - |*v*| is the difference of volumes in a particular direction. Thus, it can be noted that variogram range of each nested structure increases as the size of the volume *V* increases.

2. The variance contributions C_v^m, of each nested structure $\gamma_V^m(\mathbf{h}), \quad m = 1,\ldots,k,$ change from the small scale to the large scale as follows

$$C_V^m = C_v^m \frac{1 - \bar{\gamma}^m(V,V)}{1 - \bar{\gamma}^m(v,v)} \tag{4}$$

Where $\bar{\gamma}^m(V,V)$ and $\bar{\gamma}^m(v,v)$ are the average variogram or "gamma-bar" values. In particular, $\bar{\gamma}^m(V,V)$ represents the mean variogram $\gamma^m(\mathbf{h})$ when one extremity of the vector **h** describes the domain *V* and the other extremity of this vector independently describes the same domain. The values of gamma-bar's rarely can be calculated analytically; therefore, they are usually estimated numerically by volume discretization, that is.

$$\bar{\gamma}^m(V,V) = \frac{1}{V}\frac{1}{V}\int_V\int_V \gamma^m(\mathbf{y}-\mathbf{y}')d\mathbf{y}d\mathbf{y}' \approx \frac{1}{n}\frac{1}{n}\sum_{i=1}^{n}\sum_{j=1}^{n}\gamma^m(\mathbf{u}_i-\mathbf{u}_j) \tag{5}$$

Where *n* is the number of regular spaced points discretizing the volume *V*.

3. The nugget effect C_V^0 at the volume support *V* is given by:

$$C_V^0 = C_v^0\frac{|v|}{|V|} \tag{6}$$

If the small volume *v* is a point scale, then the nugget effect of the upscaled semivariogram is zero.

These scaling laws require certain assumptions for its implementation. Those assumptions are: 1) the shape of each individual semivariogram nested structure (i.e., exponential, spherical) does not change in the upscaling. That is shape of each nested structure is assumed to be scale invariant; 2) the averaging is performed with non-overlapping volumes; and 3) the variables scale in a linear fashion.

Direct Semivariogram Upscaling (DSU)

Direct variogram upscaling approach is a new theoretically derived approach for variogram upscaling. Babak and Leuangthong (2008) showed that if $\gamma_v(\mathbf{h})$ is a semivariogram model at a point support (given by (3)), then the semivariogram $\gamma_V(\mathbf{h})$ at the block support *V* can be calculated as:

$$\gamma^V(\mathbf{h}) = \sum_{m=1}^{k} C^m\left[\bar{\gamma}^m(V,V_{\mathbf{h}}) - \bar{\gamma}^m(V,V)\right] \tag{7}$$

where $V_{\mathbf{h}}$ denote the support *V* translated from *V* by the vector **h**; $\bar{\gamma}^m(V,V_{\mathbf{h}})$ represents the average of each nested variogram structure $\gamma^m(\mathbf{h})$ when one extremity of the vector **h** describes the support *V* and the other extremity independently describes the translated support $V_{\mathbf{h}}$, that is,

$$\bar{\gamma}_v^m(V,V_{\mathbf{h}}) = \frac{1}{V}\frac{1}{V}\int_V\int_V \gamma^m(\mathbf{w}-(\mathbf{x}+\mathbf{h}))d\mathbf{w}\,d\mathbf{x} \tag{8}$$

Since there is no analytic solution for calculating average semivariograms for any of the commonly used variogram models, they are calculated through numerical integration (11):

$$\bar{\gamma}^m(V,V_{\mathbf{h}}) \approx \frac{1}{n}\frac{1}{n}\sum_{i=1}^{n}\sum_{j=1}^{n}\gamma^m(\mathbf{u}_i-(\mathbf{u}_j+\mathbf{h})) \tag{9}$$

The upscaled semivariogram model is then obtained as:

$$\gamma^V(\mathbf{h}) = \sum_{m=1}^{k} C^m \left[\bar{\gamma}^m(V, V_{\mathbf{h}}) - \bar{\gamma}^m(V, V) \right]$$
$$\approx \sum_{m=1}^{k} C^m \left[\frac{1}{n}\frac{1}{n} \sum_{i=1}^{n}\sum_{j=1}^{n} \gamma^m(\mathbf{u}_i - (\mathbf{u}_j + \mathbf{h})) - \frac{1}{n}\frac{1}{n} \sum_{i=1}^{n}\sum_{j=1}^{n} \gamma^m(\mathbf{u}_i - \mathbf{u}_j) \right] \quad (10)$$

Note from (7)-(10) that, on the contrary to scaling law, the direct upscaling approach does not make any unrealistic simplifying assumptions about the variogram shape invariance or averaging of non-overlapping volumes.

Comparison between Scaling Laws versus Direct Semivariogram Upscaling

Four simulation studies are undertaken to compare the performance of the variogram scaling laws and direct variogram upscaling approach in predicting the variograms at larger block supports. Each study corresponds to different simulation in terms of different point support variograms, different geomodel size, presence of anisotropy, availability of conditioning data, ect. In particular simulation studies 1 and 2 present results of the performance of SLL and DSU in predicting variograms at a block support reproduced by unconditional simulation with isotropic and anisotropic variograms, respectively; while studies 3 and 4 are based on real data and subsequently deal with conditional simulation. Data for conditional simulation are assumed to be at a pseudo-point scale.

Each simulation study is conducted as follows. Full grids of nodes are generated using sequential Gaussian simulation (SGS) using a particular variogram model and conditioning data if applicable. Reproduction of the variogram at a pseudo point scale support is carefully checked. Then simulated realizations are upscaled to different pre-selected block sizes. Average experimental variograms are calculated at chosen block supports and compared to the variogram obtained by scaling laws and variogram obtained by direct variogram upscaling approach. The difference between both methods variograms and the average variogram are evaluated based on the mean absolute error criterion.

Unconditional 1D case

This 1D example is chosen small enough to easily visualize the results yet large enough to show realistic variations in the results. The 1D case can be thought of as an analogy to one well or exploratory borehole for petroleum and mining, respectively. The conclusions drawn from this example are considered reasonably general.

An unconditional 1D SGS simulation is applied to generate 100 realizations of 1000 simulated nodes each with a separation distance of 1 unit between neighboring nodes. Simulation is performed using an isotropic spherical variogram model $\gamma(\mathbf{h})$ given by:

$$\gamma(\mathbf{h}) = 0.20 + 0.50 Sph_{75}(\mathbf{h}) + 0.30 Sph_{140}(\mathbf{h}) \quad (11)$$

Subsequently, simulated realizations are upscaled to three different blocks sizes: 10, 20 and 50 points each (see Figure 2).

Results of SLL and DSU in fitting the average experimental variogram at different block supports are shown in Figure 2. It can be noted that for all three upscaled block sizes, the direct semivariogram upscaling (DSU) approach, as expected, predicts very well all upscaled variograms. Unfortunately, the same can note be said about the scaling laws approach. The departure between average experimental variograms and variograms obtained by upscaling using scaling laws becomes even more pronounced with increase in the block size, see Figure 2. Table 1 shows the mean absolute error of the two semivariogram upscaling approaches in fitting the average experimental variogram values.

Table 1: Mean absolute error of SLL and DSU in fitting the average experimental variogram values at a block size of 10, 20 and 100 cells.

Point Scale	10 cells	20 cells	100 cells

	SL	DSU	SL	DSU	SL	DSU
0.0065	0.0198	0.0149	0.0229	0.0077	0.0245	0.0127

Note from Table 1 that for small upscaling volumes such as the 10 cells, the DSU and SLL both perform well; however, the DSU approach outperforms the SLL by 30%. With increase in the upscaling volume, the outperformance of DSU approach over SLL increases even more. For the upscaling volume of 20 cells the DSU fitting is almost 300% better than that of the SL approach. Similar conclusions can be made for the upscaling volume of 100 cells.

Unconditional 2D case

To show that direct variogram upscaling outperforms variogram scaling laws equally well in higher dimensions and in the case of anisotropy, another example of unconditional simulation is considered. Sequential Gaussian simulated is applied to generate 25 realizations of the area of 256 by 256 grid blocks of size 1 by 1 unit using a semivariogram model consisting of three structures - a nugget effect of 0.30 and two anisotropic spherical models with contributions of 0.25 and 0.45:

$$\gamma(\mathbf{h}) = 0.30 + 0.25 Sph_{\substack{Major:50 \\ Minor:25}}(\mathbf{h}) + 0.45 Sph_{\substack{Major:80 \\ Minor:40}}(\mathbf{h}) \qquad (12)$$

Simulated realizations are then upscaled to three different block sizes: 4 by 4, 8 by 8 and 32 by 32 units. As before, we compare average experimental variograms obtained in simulation to the upscaled variograms obtained by direct upscaling approach and variogram scaling laws.

Figure 3 shows results of simulation and block upscaling. For all three upscaled block sizes, the direct variogram upscaling (DSU) approach produces upscaled variogram models that are in very close agreement with average experimental variogram models. Scaling laws, on the other hand, only predict well upscaled variograms when the change in the block size is minimal (see Figure 3); when the block size increases, the departure between variograms predicted by SL and average experimental variograms becomes more and more significant.

To quantify the performance of DSU and SL more formally, the mean absolute error is used. Results for the mean absolute error obtained in each case are shown in Table 2. Note the mean absolute error was calculated based on 100 distance units in the major continuity direction and 80 distance units in the minor continuity direction.

Table 2: Mean absolute error of SL and DSU in fitting the average experimental variogram values at a block size of 4 by 4, 8 by 8 and 32 by 32 units.

	Pseudo-point Scale	4 x 4		8 x 8		32 x 32	
		SL	DSU	SL	DSU	SL	DSU
Major (Azimuth 90˚)	0.0159	0.0274	0.0197	0.0223	0.0116	0.0286	0.0148
Minor (Azimuth 0˚)	0.0090	0.0221	0.0177	0.0131	0.0046	0.0172	0.0044

It can be noted from Table 2 that the DSU approach fits the average experimental variogram values at different block sizes by far better than SLL approach. Again it must be noted that the fitting behavior of both upscaling approached is similar when the upscaling volume is small; the difference in variogram DSU and SLL predictions increases as the upscale size is bigger. Specifically, for the block sizes of 8 by 8 and 32 by 32 units, the SLL results in almost twice larger mean absolute error as that of the DSU.

Amoco Example

The following example is based on Chu and Xu (1995). A 10500 by 10500 ft^2 reservoir layer is considered, with 62 wells in the study area (Figure 4). The variable of interest is porosity (averaged along the wells). The horizontal variogram of the normal score transformed porosity in the direction of major and minor continuity is shown in Figure 5 and given below (13):

$$\gamma(\mathbf{h}) = 0.18 Sph_{\substack{Major:1200 \\ Minor:5000}}(\mathbf{h}) + 0.82 Sph_{\substack{Major:25000 \\ Minor:5000}}(\mathbf{h}) \quad (13)$$

Let us now compare the direct variogram upscaling and variogram scaling laws in predicting the upscaled variograms in the presence of conditional data in 2D. 50 realizations are simulated using SGS on a grid of 105 by 105 cells; each cell represents an area of 100 by 100 square feet (pseudo point scale). Resulting simulated maps are upscaled to two different scales: blocks of size 5 by 5 cells and 15 by 15 cells. Figure 6 shows the comparison of the average experimental variograms of the upscaled realizations with variograms obtained by two upscaling approaches, that is, DSU and SLL. It can be noted that the direct upscaling approach outperforms the scaling laws approach in predicting/fitting the average experimental semivariogram values of the upscaled volumes for both block support sizes, that is, 5 by 5 and 15 by 15 cells, respectively, in both major and minor direction of continuity. It is also worth mentioning that for the block size of 15 by 15 cells, both DSU and SLL upscaling approaches predicted that the normal score transformed porosity is less continuous than it really is in the direction of major anisotropy (SLL and DSU semivariogram models are both above the average experimental semivariogram). However, the departure of DSU variogram from the average experimental variogram is substantially smaller than that of SLL variogram. Results for the mean absolute error for SLL and DSU variograms are given in Table 3. Again note the significant outperformance of the DSU over the SLL approach. Note also that for the minor anisotropic range the mean absolute error was calculated based on all lag distances less than 4000 feet; this is of a trend reproduced by simulation in that direction.

Table 3: Mean absolute error of SLL and DSU in fitting the average experimental variogram values at a block size of 5 by 5 and 15 by 15 units.

	Pseudo-point Scale	**5x5**		**15x15**	
		SL	**DSU**	**SL**	**DSU**
Major (Azimuth 90˚)	0.0138	0.0314	0.0152	0.0738	0.0356
Minor (Azimuth 0˚)	0.0341	0.0504	0.0356	0.1298	0.0777

3D Porphyry Example

The fourth exercise is based on a 3D porphyry data set consisting of 2376 samples collected over a volume of a size 400 by 600 by 140 cubic meters. The semivariogram model of the normal score transformed porphyry is given below:

$$\gamma(\mathbf{h}) = 0.10 + 0.20 Sph_{\substack{major:60 \\ minor:50 \\ vertical:60}}(\mathbf{h}) + 0.35 Sph_{\substack{major:160 \\ minor:160 \\ vertical:300}}(\mathbf{h}) + 0.35 Sph_{\substack{major:1000 \\ minor:240 \\ vertical:350}}(\mathbf{h}) \quad (14)$$

For this exercise 20 SGS realizations are generated at a resolution of 100 by 150 by 70 cells of size 32 units^3 each; simulated realizations are then upscaled to two block sizes: 20 by 30 by 14 and 10 by 15 by 7 cells, respectively. Selected block sizes correspond to averaging of 5 by 5 by 5 and 10 by 10 by10 cells in simulated realizations.

Figure 9 shows results of SLL and DSU in fitting the average experimental variogram at the two chosen block supports. Figure 9 also shows reproduction of the initial pseudo-point support variogram by simulation. It can be noted that the pseudo-point support variogram is fairly well reproduced but slightly shifted in the vertical direction (see Figure 9). Results for the mean absolute error for SLL and DSU variograms are given in Table 4. Again note that for all upscaling volume sizes, the DSU approach produces much better results than the SLL approach.

Table 3: Mean absolute error of SLL and DSU in fitting the average experimental variogram values at block discretizations of 5 by 5 by 5 and 10 by 10 by 10 cells.

	Initial	**5x5x5**	**10x10x10**

	Semivariogram Model	SL	DSU	SL	DSU
Major 0˚ Azimuth	0.0332	0.0335	0.0268	0.0307	0.0201
Minor 90˚ Azimuth	0.0441	0.0414	0.0405	0.0409	0.0361
Vertical -90˚ Dip	0.0332	0.0475	0.0283	0.0529	0.0236

Conclusions

In this paper two different approaches for variogram upscaling are compared. These approaches are direct variogram upscaling (DSU) approach and scaling laws (SLL). It is shown through a number of simulation studies that DSU performs by far better than the SLL in fitting the average experimental variogram values at any block size. Moreover, it is also shown that with increase in the block size, outperformance of direct variogram upscaling over scaling laws significantly increases. Thus, DSU should be preferred over SLL for predicting upscaled variograms especially when the upscaling volume is large compared to the scale of data.

References

Babak O, Leuangthong, O (2008) Direct Upscaling of Variograms and Cross Variograms for Scale Consistent Geomodeling. Centre of Computational Geostatistics, Report 10.

Frykman P, Deutsch C V (2002) Practical application of geostatistical scaling laws for data integration. Petrophysics 43:153-171

Frykman P, Deutsch C V (1999) Geostatistical scaling laws applied to core and log data. SPE 56822

Journel A G, Huijbregts C J (1978) Mining geostatistics. Academic Press, London

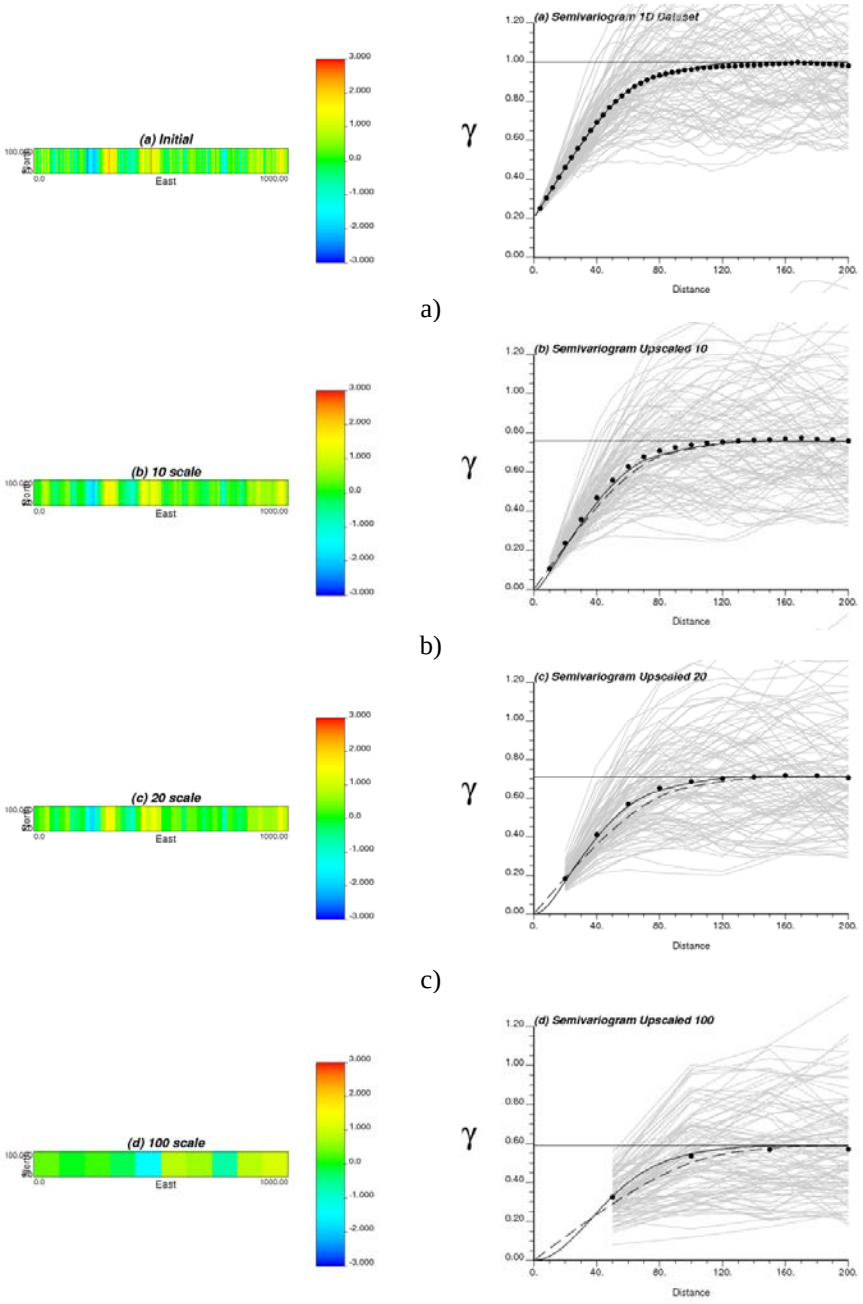

Figure 2: Variograms obtained by scaling laws (dashed lines) and direct variogram upscaling (solid lines) for (a) a point scale, (b) block of 10 points, (c) block of 20 points, and (d) block of 100 points. Experimental semivariograms of realizations and average experimental semivariograms are shown in gray lines and dots, respectively.

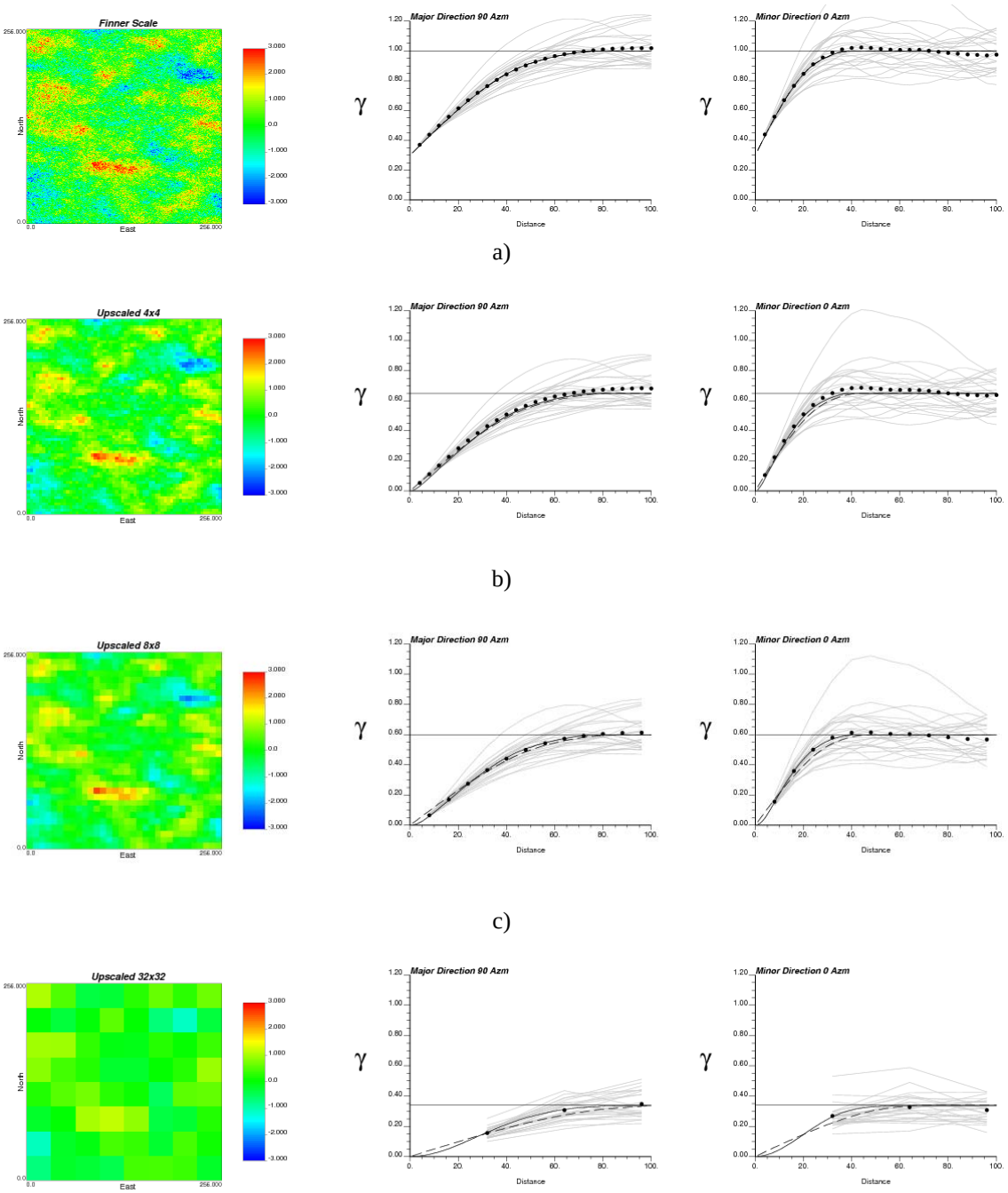

Figure 3: Example unconditional SGS realization along with respective block upscaled realizations (left) and variograms in the direction of major (middle) and minor (right) continuity obtained by scaling laws (dashed lines) and direct variogram upscaling (solid lines) for (a) a pseudo-point scale, (b) block of size 8 by 8 cells, and (c) block of size 32 by 32 cells. Experimental semivariograms of realizations and average experimental semivariograms are shown in gray lines and dots, respectively.

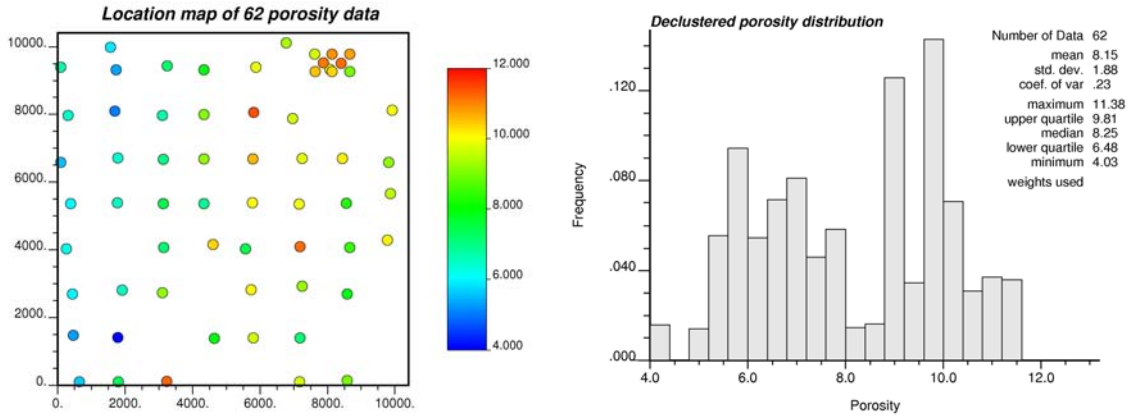

a) b)

Figure 4: Location map of porosity (a) and representative (declustered) porosity distribution (b). Results are in original units.

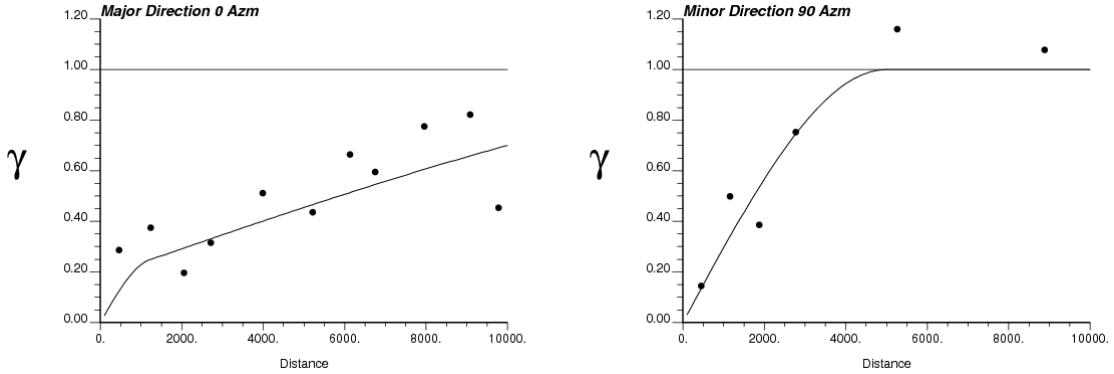

Figure 5: Experimental variogram (dots) and its theoretical fit in the direction of major (left) and minor (right) continuity of the normal score transformed porosity.

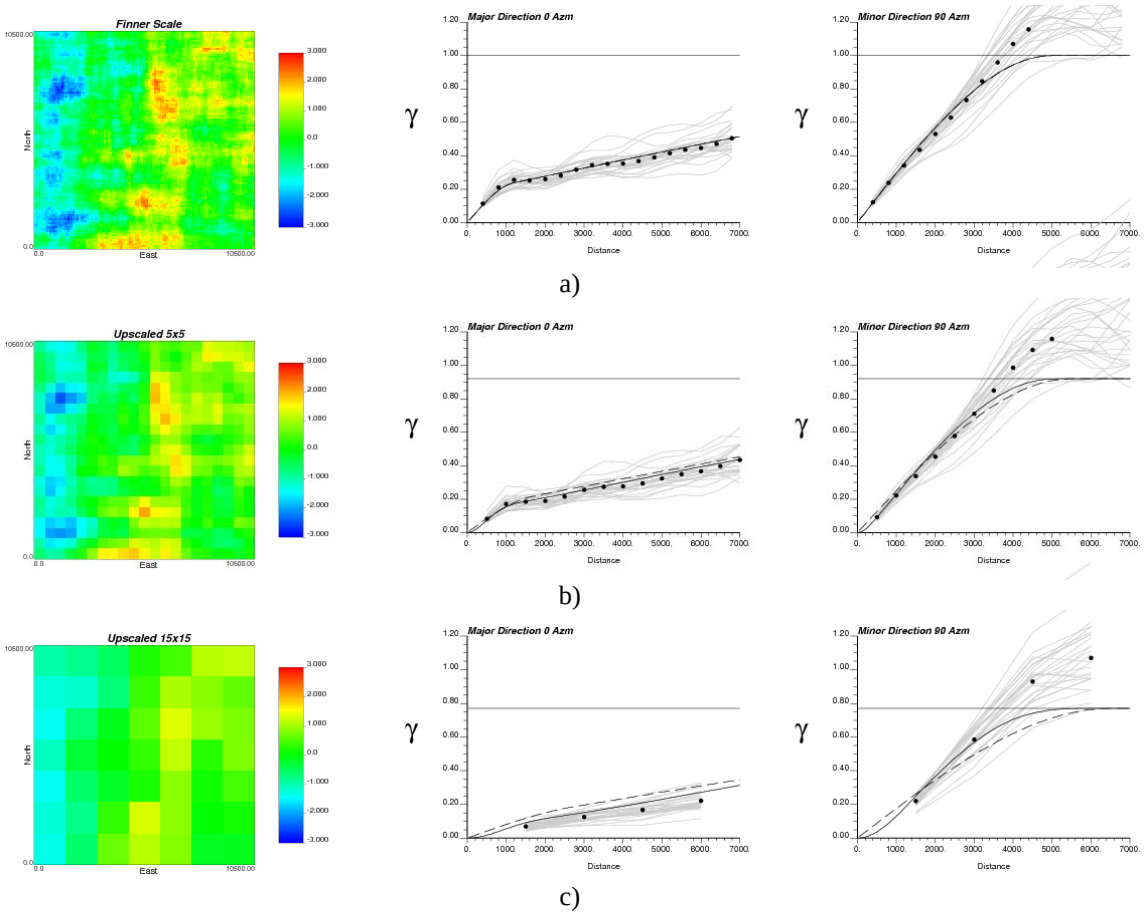

Figure 6: Example SGS realization along with respective block upscaled realizations in normal score units (left) and variograms in the direction of major (middle) and minor (right) continuity obtained by scaling laws (dashed lines) and direct variogram upscaling (solid lines) for (a) a pseudo-point scale, (b) block of 5 by 5 cells and (c) block of 15 by 15 cells. Experimental semivariograms of realizations and average experimental semivariograms are shown in gray lines and dots, respectively.

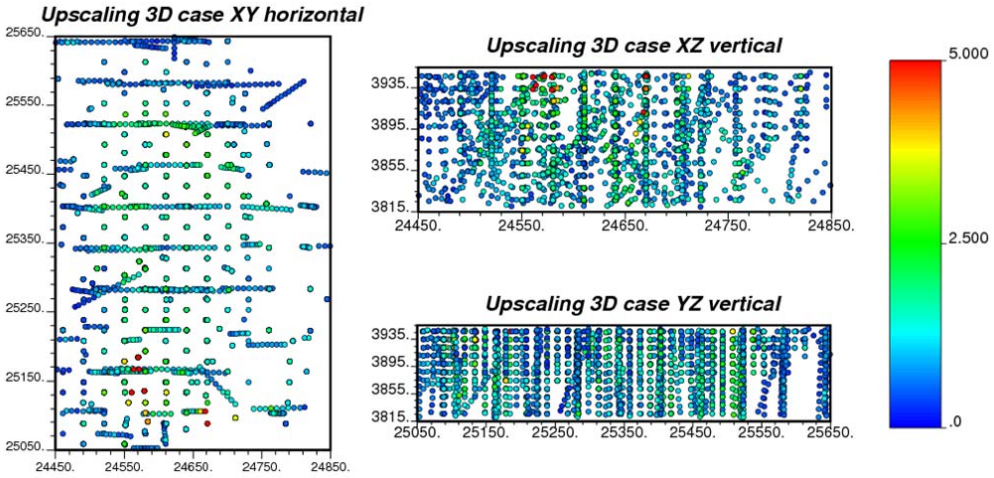

Figure 7: Location map of copper grades.

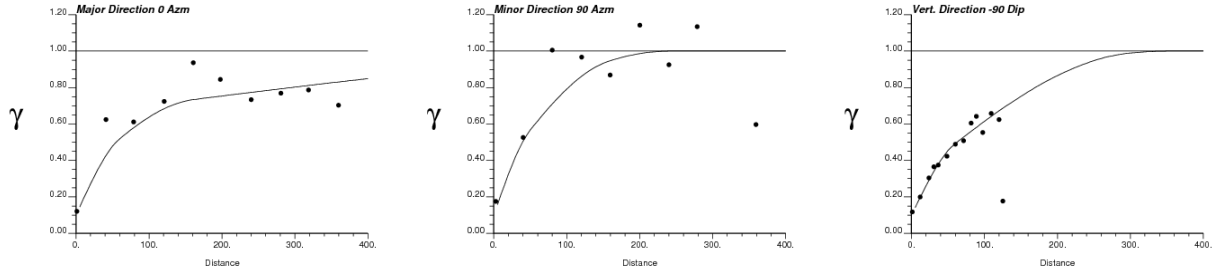

Figure 8: Experimental variogram (dots) and its theoretical fit in the direction of major (left), minor (middle) and vertical (right) continuity of the normal score transformed copper grade.

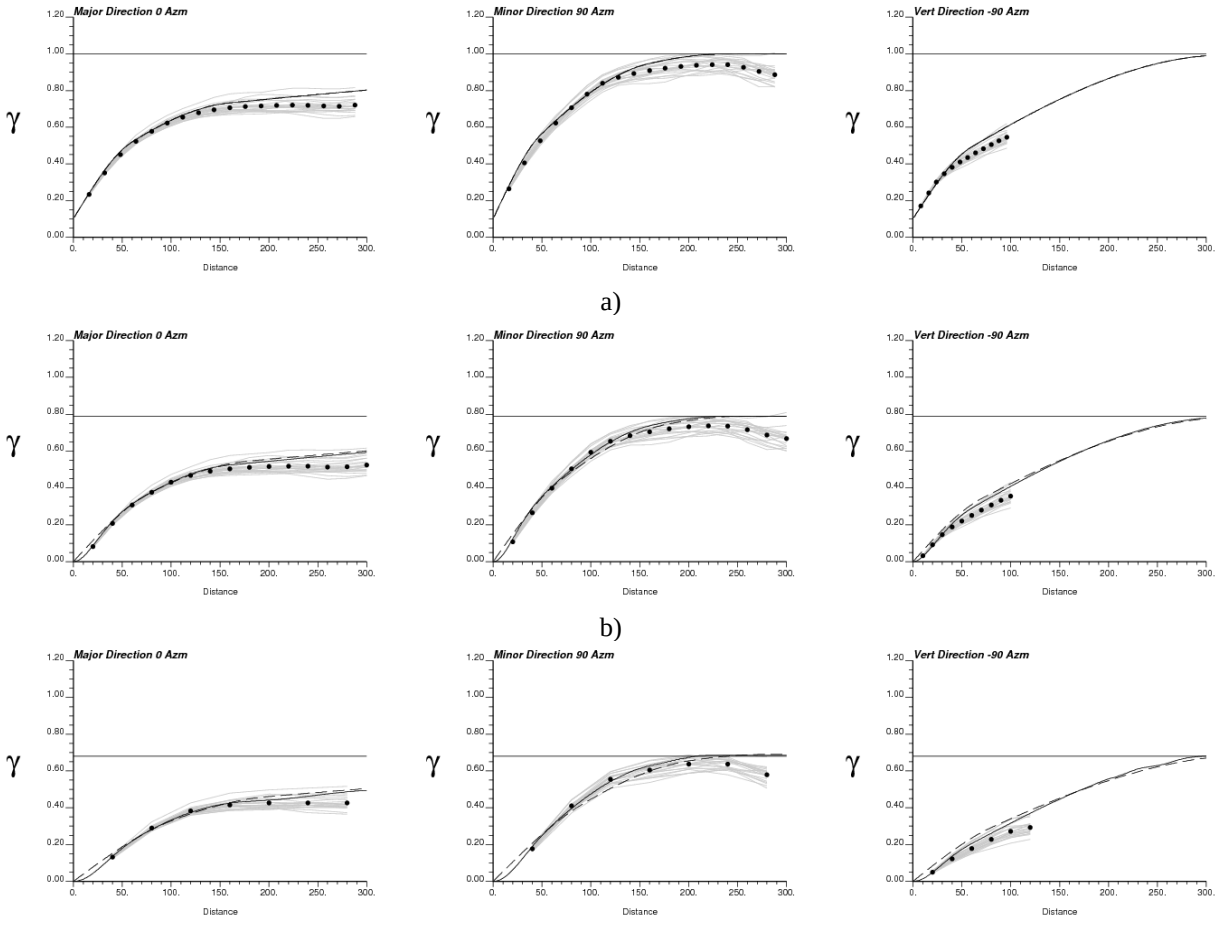

a)

b)

c)

Figure 9: Variograms in the direction of major (left), minor (middle) and vertical (right) continuity obtained by scaling laws (dashed lines) and direct variogram upscaling (solid lines) for (a) a pseudo-point scale, (b) block of 5 by 5 by 5 cells and (c) block of 10 by 10 by 10 cells. Experimental semivariograms of realizations and average experimental semivariograms are shown in gray lines and dots, respectively.